NOAA Technical Memorandum OAR PMEL-138

UPPER OCEAN WARMING: SPATIAL PATTERNS OF TRENDS AND INTERDECADAL VARIABILITY

D.E. Harrison[1,2,3]
Mark Carson[2,3]

[1]Pacific Marine Environmental Laboratory
Seattle, WA

[2]Joint Institute for the Study of the Atmosphere and Ocean (JISAO)
University of Washington, Seattle, WA

[3]School of Oceanography
University of Washington, Seattle, WA

Pacific Marine Environmental Laboratory
Seattle, WA
January 2008

UNITED STATES DEPARTMENT OF COMMERCE

Carlos M. Gutierrez
Secretary

NATIONAL OCEANIC AND ATMOSPHERIC ADMINISTRATION

VADM Conrad C. Lautenbacher, Jr.
Under Secretary for Oceans and Atmosphere/Administrator

Office of Oceanic and Atmospheric Research

Richard W. Spinrad
Assistant Administrator

NOTICE from NOAA

Mention of a commercial company or product does not constitute an endorsement by NOAA/OAR. Use of information from this publication concerning proprietary products or the tests of such products for publicity or advertising purposes is not authorized. Any opinions, findings, and conclusions or recommendations expressed in this material are those of the authors and do not necessarily reflect the views of the National Oceanic and Atmospheric Administration.

Contribution No. 3144 from NOAA/Pacific Marine Environmental Laboratory

Also available from the National Technical Information Service (NTIS)
(http://www.ntis.gov)

Contents

Upper ocean warming: Spatial patterns of trends and interdecadal variability

D.E. Harrison[1,2,3], and M. Carson[2,3]

Abstract. Extending previous work, long-term temperature trends in the upper layers of the ocean are calculated from gridded observed data to explore spatial and temporal trend variability. Interdecadal and spatial trend variability is presented for various analysis region sizes. Depths between 50 m and 1000 m are examined. Despite using larger grid boxes, most of the ocean does not have 50-year trends that are significant at the 90% confidence level. At 100 m, only about 35% of the ocean has such trends and the coverage declines dramatically with increasing depth. As noted before there is much spatial structure in 50-year trends, with areas of strong warming and strong cooling. There is also strong interdecadal variability shown in 20-year trends; almost every region studied shows both warming and cooling 20-year trends over a 50-year period. 50-year trend results are compared and contrasted with trends calculated from data interpolated to standard levels and from a dataset used in previous heat content trend studies. These comparisons show that different data treatments can yield significantly different trends. Thus, the uncertainty in heat content integrals is large and such integrals may not be truly representative of the global ocean heat content. This situation prevails because of the presence of strong interdecadal and spatial trend variability in conjunction with strong temporal and spatial sampling issues. It is suggested that calculating a world ocean residual heat content trend is highly problematic over this period.

1. Introduction

There is great interest in the extent to which there is large-scale, low-frequency variability in oceanic temperature and heat content, regionally and over the world ocean. Attempts have been made to quantify long-term temperature or heat content trends on global and basin scales (e.g., Levitus *et al.*, 2000, 2005; Gille, 2002; Willis *et al.*, 2004; Lyman *et al.*, 2006; Gouretski and Koltermann, 2007). Many of the methods employed involve averaging temperature anomalies (or volume-integrating heat content anomalies) over wide depth ranges and averaging all data globally, zonally, or within a basin, usually to beat down noise and obtain a residual temperature signal (residual in the sense that, after integrating, all changes due to advective or diffusive movement of heat are averaged out). Averaging anomalies over large regions and depth ranges, while presumably resulting in a residual answer, does not reveal the spatial character of temperature trends in the ocean, and is problematic, especially given the sampling discrepancies in time (early record vs. late record sampling rates) and space (both laterally—Northern Hemisphere vs. Southern Hemisphere, and in depth—upper ocean vs. deep ocean). Previously, some long-term temperature trend spatial features have been presented regionally: for the North Atlantic as plan view, and basin-wide and global time series in Levitus *et al.* (1994, 2000); basin-wide as zonal average vs. depth in Levitus *et al.* (2005, supplementary material

[1]NOAA, Pacific Marine Environmental Laboratory, Seattle, WA
[2]Joint Institute for the Study of the Atmosphere and Ocean (JISAO), University of Washington, Seattle, WA
[3]School of Oceanography, University of Washington, Seattle, WA

at `http://www.nodc.noaa.gov/OC5/DATA_ANALYSIS/heat\_intro.html`); and basin-wide and global time series with depth in Barnett *et al.* (2005) and Pierce *et al.* (2006). In this paper we attempt to estimate trends while leaving as much spatial and temporal information available as possible, and also to understand what regions are not sampled enough for trend estimation. Further, we apply our analysis methods to different data treatments to test the sensitivity of trends to various data processing methods.

To explore the horizontal and vertical spatial scales of temperature trends in the upper ocean, we originally took raw data from World Ocean Database 2001 (Conkright *et al.*, 2002, hereafter WOD01), and gridded the data into $1^\circ \times 1^\circ$ and $2^\circ \times 2^\circ$ datasets at three discrete depths (100, 300, and 500 m), making daily and monthly averages for the time grids. The analysis was only applied to regions that satisfied a temporal data distribution requirement to increase the likelihood that calculated trends were representative of long-term trends. As a result, much of the southern ocean regions were excluded. Without removing any climatology and with no further averaging or infilling of the datasets, maps of trend magnitudes were calculated which demonstrated the spatial variability and vertical structure of temperature trends over a 51-year period, January 1950 to December 2000. These results, along with maps of 20-year trends showing the spatial character of the interdecadal variability of the trends, were published recently (Harrison and Carson, 2007, hereafter HC).

In the present paper, data are binned and averaged into larger grid boxes to examine the effects of grid box size, and to attempt to characterize the trend magnitude and variability in southern ocean regions. The dataset used is the newer World Ocean Database 2005 (Boyer *et al.*, 2006, hereafter WOD05), which increased the total number of stations—7,900,349 compared to 7,037,213 in WOD01 (Conkright *et al.*, 2002). Data were also gathered at the additional depths of 50 m, to better characterize the uppermost subsurface layer, and 700 and 1000 m to examine the data distribution and trends at deeper depths. Monthly anomalies were calculated and used in place of raw data due to the presence of horizontal temperature gradients in larger boxes and to remove seasonal effects. Also, overlapping 20-year trends were calculated at a larger resolution to provide better coverage of the ocean (with more grid boxes passing a minimal data distribution requirement for trend calculation) and are included for exploring interdecadal variability.

In addition to extending the results from HC, trends from the dataset analyzed in Levitus *et al.* (2005) were compared to the trends calculated from observed- and standard-level data from WOD05. This objectively analyzed dataset of annual anomalies calculates different long-term temperature trends than both observed- and standard-level data trends in many regions, and obfuscates the level of uncertainty in trends in the southern ocean regions. Standard-level data available in WOD05 has also been processed with the same analysis methods to test yet another treatment of the same data, here the interpolation of data to standard depth levels.

The methods and data used are discussed further in section 2. Section 3 contains the planview maps of 51-year (1950–2000), 49-year (1955–2003), and overlapping 20-year trend magnitudes as well as comparisons to

standard-level data trends and the Levitus *et al.* (2005) dataset. A summary and discussion of these results are presented in section 4.

2. Data and Methods

The basic analysis methods of HC are used here with some modifications. The primary dataset is the more recent World Ocean Database 2005 (Boyer *et al.*, 2006; WOD05), although data from WOD01 were also analyzed using these methods. There were few differences in the results based on these two datasets, and the results here focus on the WOD05 trends.

The HC analysis, which focused on results based on averaging data over $2^\circ \times 2^\circ$ regions, is extended to larger regions—$3^\circ \times 3^\circ$, 2° latitude $\times$ 10° longitude, and $5^\circ \times 5^\circ$. Data from WOD05 were binned into these grid boxes and averaged to produce a single monthly time series for each box within the grids. As the focus remains on temperature trend behavior at discrete depths, data were binned (following the methods in HC) at 50 m $\pm$ 2.5 m, 100 m $\pm$ 5 m, 300 m $\pm$ 20 m, 500 m $\pm$ 20 m, 700 m $\pm$ 50 m, and 1000 m $\pm$ 50 m. Analysis over the larger regions requires that climatological horizontal and temporal gradients be removed before data within each region are averaged. From each individual observation (before gridding), the $1^\circ \times 1^\circ$ climatological monthly mean from World Ocean Atlas 2005 (Locarnini *et al.*, 2006; hereafter WOA05) was removed. The anomalies in each grid box were then averaged into a monthly time series. All trend results presented here are based on temperature anomalies.

The consequences of making XBT fall-rate corrections on the data in WOD05 are also investigated here. HC argued that the effects were small enough that adjustment was very unlikely to affect the spatial patterns of temperature trend or the character of the temporal patterns in the 20-year trends. The analysis here mostly confirms this, but the correction does affect estimates of the magnitude of the 20-year trends, regionally and globally averaged temperature trends, as well as the shape of regional and global time series.

Regrettably, there are a considerable number of observations for which the correction status is uncertain—about 55% of the XBTs in WOD05 are of unknown type (Boyer *et al.*, 2006). The correction was applied only to the XBTs flagged in WOD05 as needing correction.

The time series in each grid box was fitted with a trend using linear least-squares as in HC. A data sampling criterion was used again to select regions which are minimally sampled adequately through time. Here we have chosen a criterion of three or more monthly "gridded" observations for at least four of the five "decades" (123-month periods) between January 1950 and December 2000 in each grid box, and also for the five "decades" (9.8-yr periods) between January 1955 and December 2003. The reduction from the HC criterion of five observations for four of the five decadal periods was made to try to include as much of the ocean as possible where trends estimated from the gridded data are likely to be long-term trends, without adding in

too much noise. Plan-view maps were created of the trend magnitudes over the 51-year period, January 1950 to December 2000, and the 49-year period, January 1955 to December 2003, and are presented in the next section for regions passing the data distribution criterion and for those regions whose trends pass a 90% statistical confidence limit (CL). For overlapping 20-year trends, the gridded time series were broken into six intervals (January 1955 to January 1975, January 1960 to January 1980, ... January 1980 to January 2000) and trends were fit to each of these data subsets for each grid box.

To demonstrate one of the difficulties of estimating long-term trends in the ocean, the sampling distribution of the standard-level data in WOD05, after being gridded onto a $3^\circ \times 3^\circ \times 1$ month grid, is presented in Fig. 1 for five of the six analysis depths (50 m was excluded since its sampling is very similar to 100 m). The sampling per grid box is shown as the percentage of months having observations within a specified time interval, and boxes with no color having no observations. The time intervals all run from January of the first year to December of the last year with the years covered being displayed in Asia in each panel (e.g., the first interval is 1950 to 1962, the second is 1963 to 1975, etc.). We think that in order to estimate the decadal variability within these roughly decadal time intervals, at least 10% of the months in a period need to have observations, since the observations are usually not spread throughout the interval evenly. Otherwise, there is a good chance that subsampling the interannual variability, especially in regions where that is particularly strong, will yield spurious "interdecadal" signals throughout the time series. Given this guideline, it is clear that the Southern Hemisphere is undersampled even at 100 m through 1975 (except near coasts). In the first time interval, 1950–1962, significant portions of the Northern Hemisphere are not well sampled at all depths, and by 700 m, the sampling is particularly poor even through 1988. It is strongly suggested by these maps that the interdecadal variability, particularly below 300 m, is poorly sampled for the first two periods over much of the ocean, and the Southern Hemisphere is poorly sampled over most time periods and depths.

We are interested in testing our choice of data analysis against other possibilities. One different data handling method involves interpolating the data to standard levels. Since we used the observed-level data from WOD05 in this analysis, we chose to compare those results to trends based on the standard-level data available in the same dataset. The same general analysis was performed, except that we only binned the data into $3^\circ \times 3^\circ$ boxes of monthly anomalies (again using WOA05). Differences between this dataset and the observed-level dataset are discussed in the next section.

Figure 1: Percentage of months (from gridded standard-level data) having observations within the year-interval shown in Asia. For example, panel (a) shows the percentage of months where observations were made at 100 m over all months in the interval 1950 through 1962. Areas of no color contain no observations for the period. All maps are from WOD05 standard-level data on $3^\circ \times 3^\circ$ grids at 100 m (panels a–d), 300 m (e–h), 500 m (i–l), 700 m (m–p), and 1000 m (q–t). Decadal variability in any period is considered undersampled for regions having less than 10% of months observed (darker than light blue). Note that in this and subsequent figures there are reference lines drawn at 40°N, 40°S, equator, and 160°W for convenience.

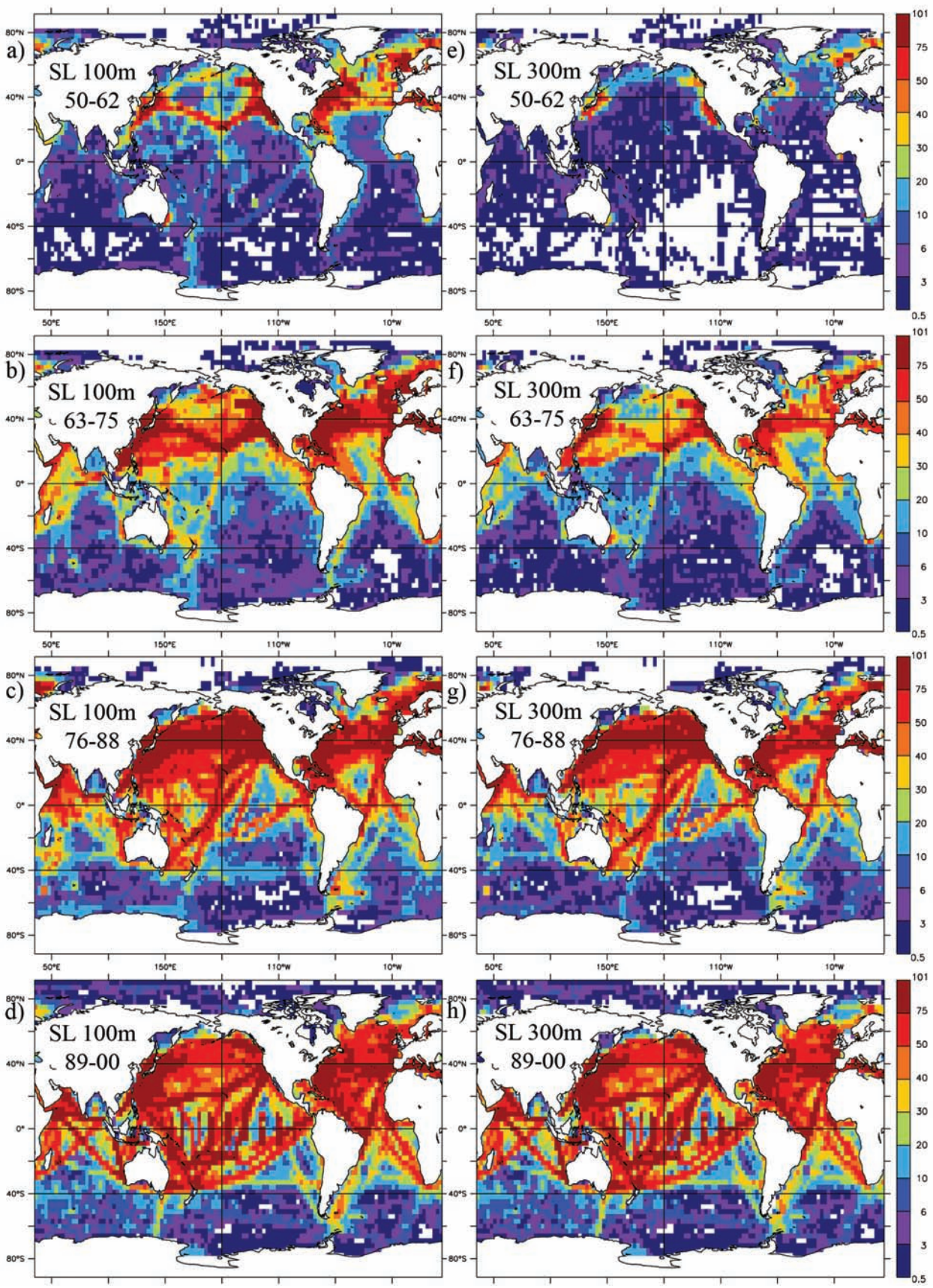
a)
SL 100m
50-62
e)
SL 300m
50-62
b)
SL 100m
63-75
f)
SL 300m
63-75
c)
SL 100m
76-88
g)
SL 300m
76-88
d)
SL 100m
89-00
h)
SL 300m
89-00
80°N
40°N
0°
40°S
80°S
50°E
150°E
110°W
10°W
101
75
50
40
30
20
10
6
3
0.5

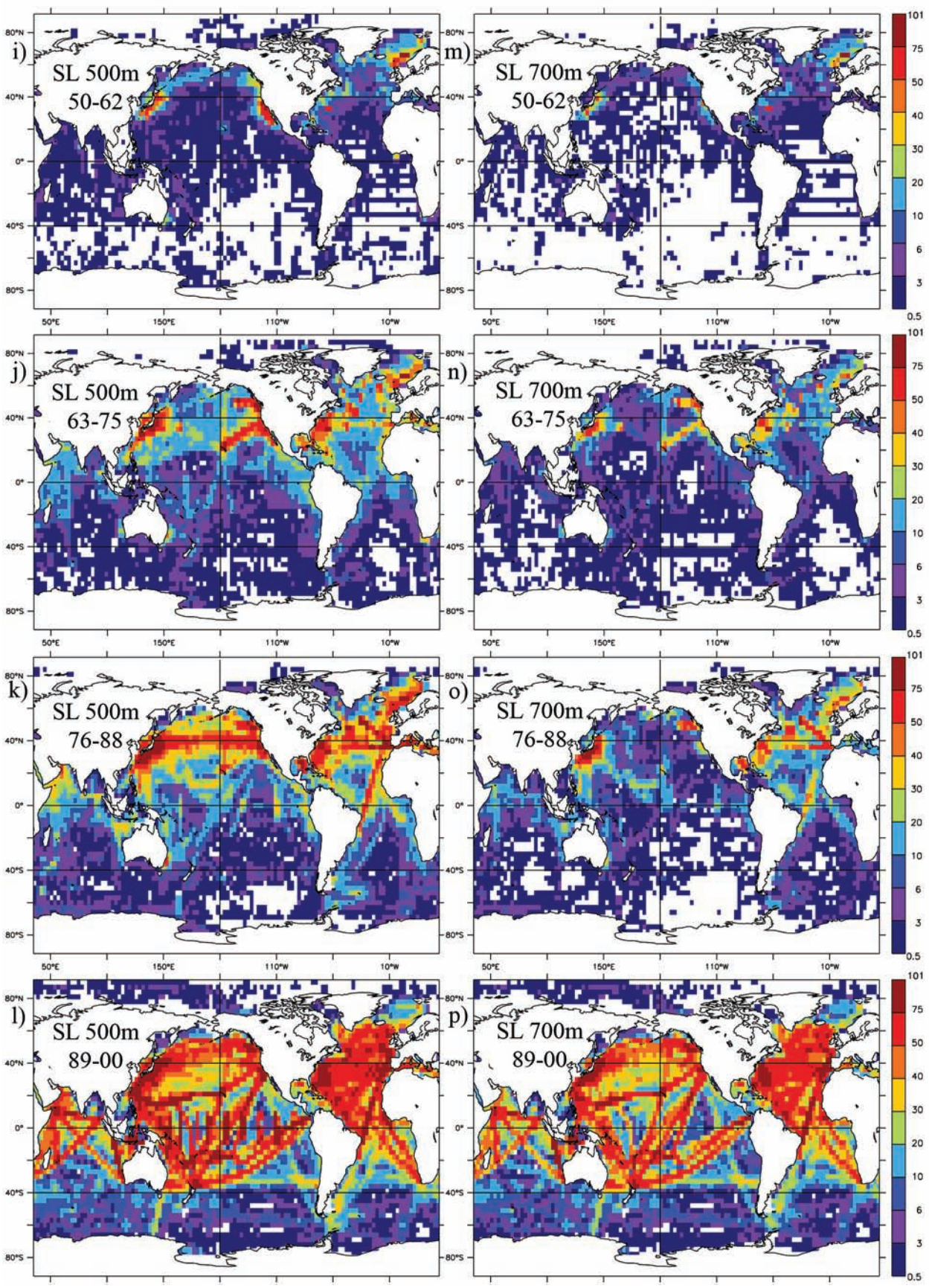
i)
SL 500m
50-62
m)
SL 700m
50-62
j)
SL 500m
63-75
n)
SL 700m
63-75
k)
SL 500m
76-88
o)
SL 700m
76-88
l)
SL 500m
89-00
p)
SL 700m
89-00
80°N
40°N
0°
40°S
80°S
50°E
150°E
110°W
10°W
101
75
50
40
30
20
10
6
3
0.5

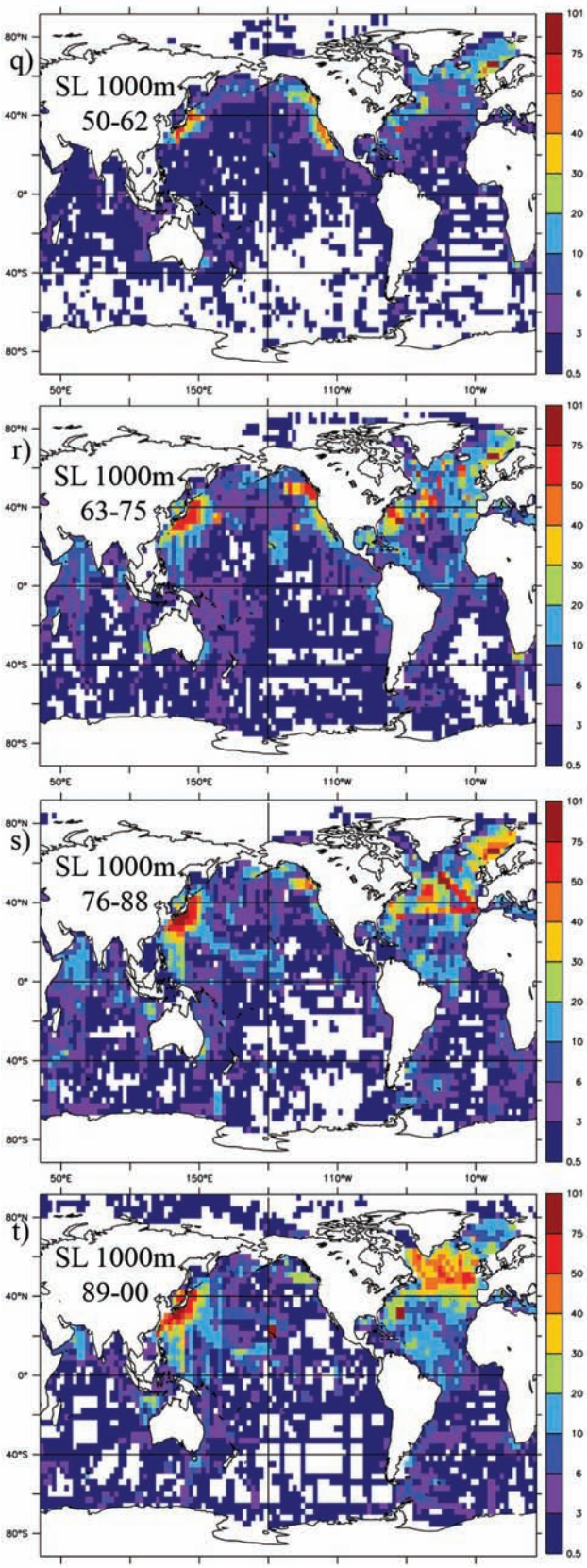
q)
SL 1000m
50-62
r)
SL 1000m
63-75
s)
SL 1000m
76-88
t)
SL 1000m
89-00
80°N
40°N
0°
40°S
80°S
50°E
150°E
110°W
10°W
101
75
50
40
30
20
10
6
3
0.5

We also compare the results of the observed- and standard-level data trends to the dataset of yearly anomalies referenced in Levitus *et al.* (2005). This data was accessed on the NODC website (`http://www.nodc.noaa.gov/OC5/DATA_ANALYSIS/anomaly_data.html`), and will be referred to hereafter as LEV05. The LEV05 dataset is an objectively analyzed, global annual anomaly dataset for each of the years covered (1955–2003) in the 16 standard levels of the upper ocean (0–700 m, defined in WOA05). This dataset was built from data in WOD01 with 310,000 additional profiles which have been included in WOD05 (Levitus *et al.*, 2005).

3. Results

3.1 1950–2000 trends from WOD05 observed-level data; effects of grid size

Maps of trend magnitudes (in °C over the 51-year period 1950–2000) are presented in Figs. 2 and 3 for 100 m and 300 m for each of the different analysis region sizes. These are based on XBT fall-rate corrected WOD05 observed-level temperature anomalies. The maps of regional trends that are statistically significant at 90% CL, based on a simple Student's t test applied to the correlation coefficient of the fitted line, reveal spatially coherent fields of trends (Fig. 2). However, trends over most of the ocean are not significant. At 100 m (Figs. 2a–d) the percent of the ocean with significant trend varies from ∼19% with $2^\circ \times 2^\circ$ regions to ∼35% with $5^\circ \times 5^\circ$ or $2^\circ \times 10^\circ$ regions; at 500 m (not shown) the corresponding range is from ∼6% to ∼24%. There are very few additional spatially coherent trend patterns revealed by using larger analysis regions. The larger area of coverage results mostly from some scattered regions in the South Indian and the tropical open ocean South Pacific, and the previous regions of significant trend just cover a larger area since the same significant trends in the smaller boxes are contained in the collocated larger ones.

In Fig. 3, the areal percentage of the ocean covered by regions passing the data distribution criterion is indicated on each map, and increases with increasing grid size. At 100 m (Figs. 3a–d) the amount of ocean with sufficient data to meet the distribution threshold increases from ∼60% with $2^\circ \times 2^\circ$ regions to ∼92% with $5^\circ \times 5^\circ$ or $2^\circ \times 10^\circ$ regions. However, the spatially coherent patterns of large-scale trend are very robust; the primary effect of increasing grid size is to smear out smaller-scale features in areas of such scales. At 300 m (Figs. 3e–h) the coverage increases from ∼34% with $2^\circ \times 2^\circ$ regions to ∼74% with $5^\circ \times 5^\circ$ or $2^\circ \times 10^\circ$ regions. There are regions

Figure 2: Temperature trends based on WOD05 observed-level anomalies over the period 1950–2000. Units are °C per 51 years, based on the linear fit trend line. Shown are regions with trends passing the 90% CL via correlation coefficient t-test at 100 m (panels a–d) and 300 m (e–h), which also pass the sampling criterion described in the text. The grid size, nominal depth, and percentage of ocean covered by significant trends are listed in Asia in each panel ($2^\circ \times 2^\circ$ in panel a, $3^\circ \times 3^\circ$ in panel b, etc.).

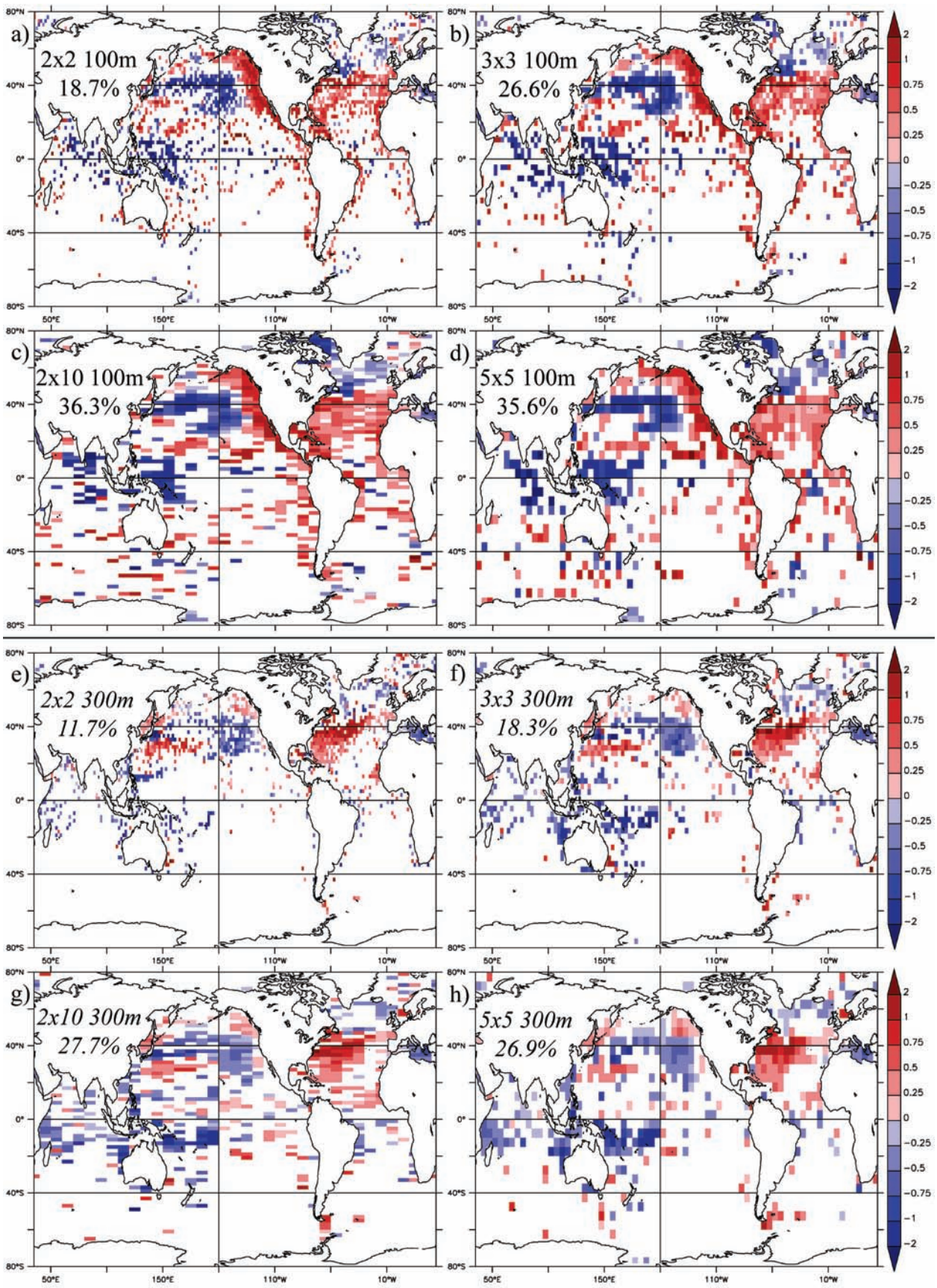
a)
2x2 100m
18.7%
b)
3x3 100m
26.6%
c)
2x10 100m
36.3%
d)
5x5 100m
35.6%
e)
2x2 300m
11.7%
f)
3x3 300m
18.3%
g)
2x10 300m
27.7%
h)
5x5 300m
26.9%
80°N
40°N
0°
40°S
80°S
50°E
150°E
110°W
10°W
2
1
0.75
0.5
0.25
0
−0.25
−0.5
−0.75
−1
−2

of spatially coherent trend revealed in the tropics by increasing the analysis region size from 2° × 2° to 3° × 3°; larger sizes do not identify additional coherent patterns. As found by HC, there are spatially structured patterns of 51-year trend, with large areas of the ocean showing warming by more than 0.75°C and other large areas showing cooling by more than 0.75°C.

Comparison of the 2° × 2° results (Figs. 2a, 2e and 3a, 3e) with those of HC (see Appendix A for 2°×2° HC results) reveals that the change of analysis approach and XBT fall rate correction do not alter the large-scale structure of the spatial patterns of temperature trends. Smaller regional patterns change only in a few places, e.g., along the southern coast of Greenland and southeast of Sumatra at 100 m (cf. Fig. 3a and Fig. 13d). However, in most places the trend magnitudes are somewhat weaker, which is due to the removal of seasonal biases, and biases between later-period uncorrected XBT and early-period MBT observations. The band along the equator present in the results from HC turned out to be due to a flaw in the copy of the WOD01 used and does not appear in the current analyses.

The variance of the trend magnitudes in these maps is much lower than in the maps presented in HC (due in large part to the removal of the seasonal cycle through calculating monthly anomalies), but even so, it is much larger than global temperature trend estimates. For the boxes passing the time data distribution requirement, the standard deviation of the trend magnitudes ranges from ∼0.61 (°C/51 yrs) to ∼0.73 (°C/51 yrs) in the two upper layers (depending on the grid box size), and from ∼0.35 (°C/51 yrs) to ∼0.49 (°C/51 yrs) in the two lower layers.

3.2 1955–2003 trends from WOD05 observed-level data; 3° × 3° grid

Trends over the 49-year interval 1955–2003 were calculated from observed-level data in WOD05 to explore trend patterns over this period, which was better sampled as reported in Levitus *et al.* (2005). The results for the 90% CL trends at all analysis depths are shown for the 3° × 3° grid in Fig. 4. Similarly, the trend results in regions passing the data distribution requirement are shown for the 3° × 3° grid in Fig. 5.

The 90% CL trends at 100 m (Fig. 4b) cover a little more of the ocean than the 1950–2000 significant trends (27.5% vs. 26.6%; compare Fig. 4b and Fig. 2b). And at 300 m (Fig. 4c), the change in coverage for significant trends is 22.5% vs. 18.3% (compare Fig. 4c and Fig. 2f). These changes are not large, but some differences in trend patterns are a bit more striking. At 100 m, the warming along the west coast of the U.S. is weaker and fewer regions are significant, but the warming in the subtropical North Atlantic and the central tropical Pacific is stronger and better featured in the later trends. The strong cooling in the western tropical Pacific and the Indian oceans are still well represented by the 1955–2003 trends. At 300 m, some

Figure 3: Same as Fig. 2, except for all regions passing the sampling criterion (at least three monthly observations per decade in at least four of the five decades of the analysis period).

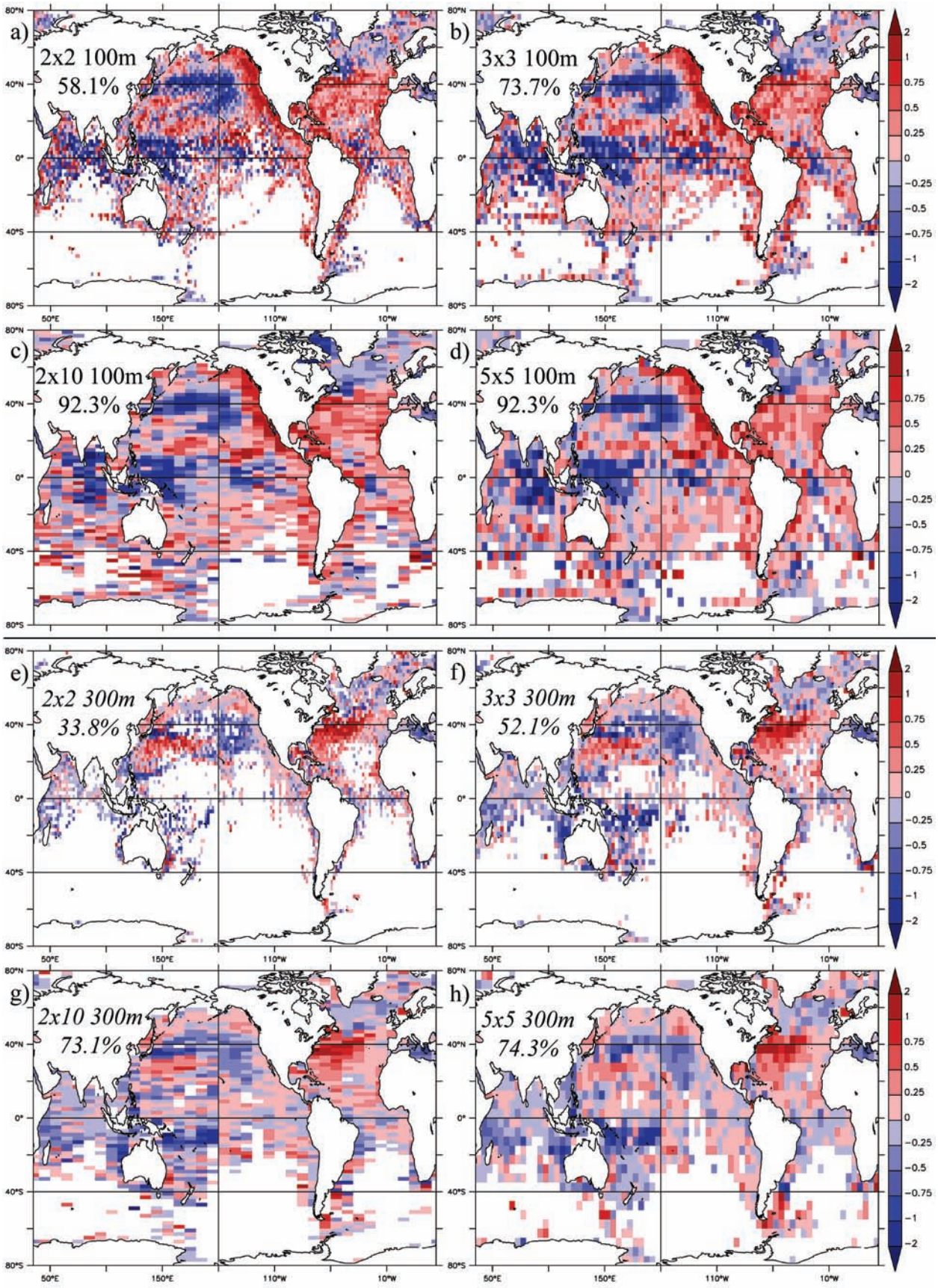
a)
2x2 100m
58.1%
b)
3x3 100m
73.7%
c)
2x10 100m
92.3%
d)
5x5 100m
92.3%
e)
2x2 300m
33.8%
f)
3x3 300m
52.1%
g)
2x10 300m
73.1%
h)
5x5 300m
74.3%
80°N
40°N
0°
40°S
80°S
50°E
150°E
110°W
10°W
2
1
0.75
0.5
0.25
0
−0.25
−0.5
−0.75
−1
−2

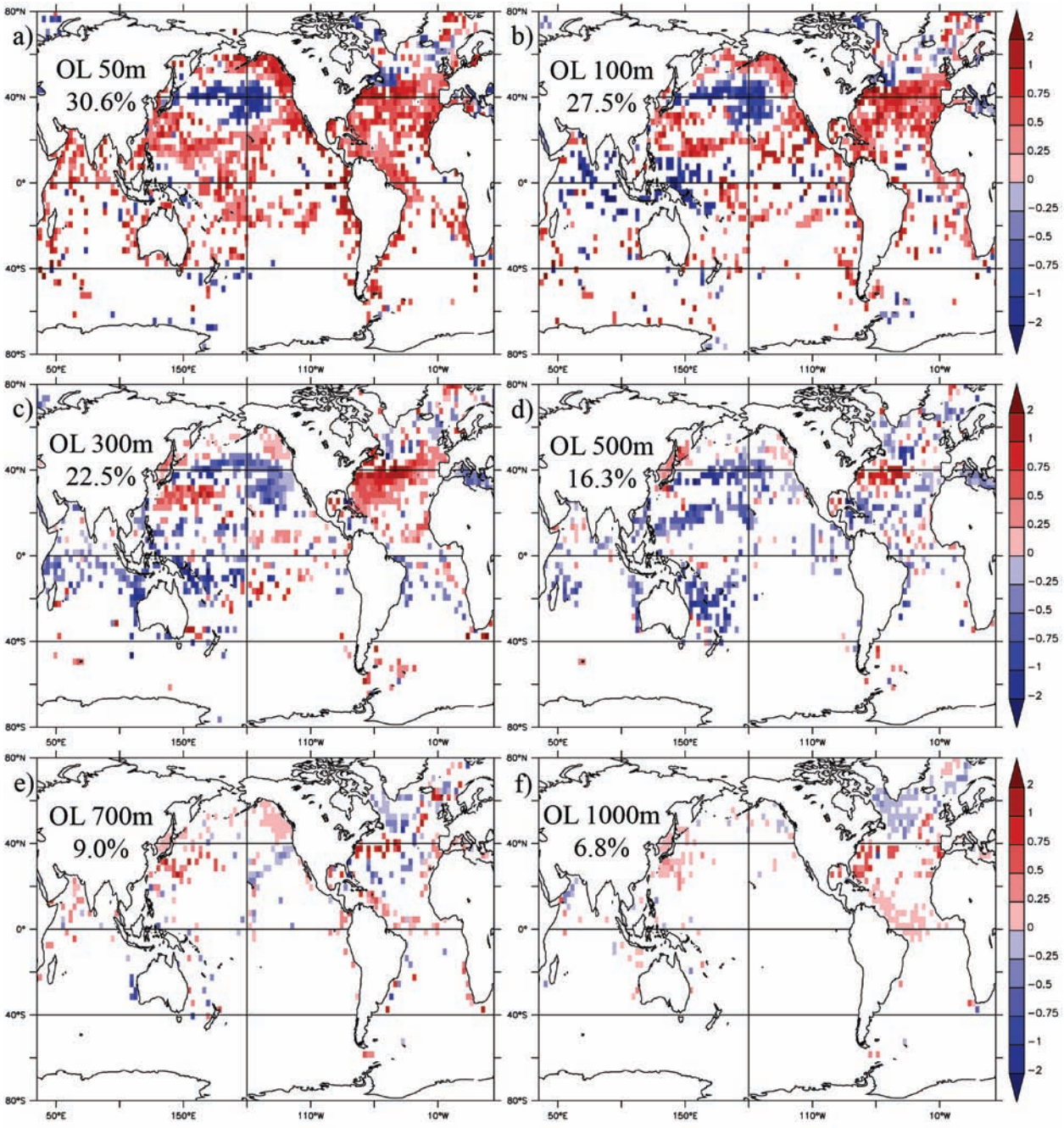

Figure 4: Temperature trends in $3° \times 3°$ regions based on WOD05 observed-level anomalies over the period 1955–2003 (units are °C per 49 years). Shown are regions with trends passing the 90% CL via correlation coefficient t-test as well as the sampling criterion. The grid size, nominal depth, and percentage of ocean covered by significant trends are listed in Asia in each panel. The color bar is the same as in Figs. 2 and 3.

new coherent features are more evident in the less-sampled tropical North Pacific, with a warming patch east of 160°W and a cooling patch west of 160°W. There is also a stronger suggestion of warming in the tropical South Pacific east of 160°W and cooling in more of the tropical/subtropical South Atlantic.

It is clear from Fig. 4 that at deeper depths the coverage of the ocean with statistically significant trends decreases with depth, especially below 460 m, which is the terminal depth of the ubiquitous T-4 XBTs. Also, for the most part, the trends at the two deepest depths, 700 and 1000 m (Figs. 4e, f), are very weak except for some strong warming near 40°N in the North Atlantic (which shows at all depths), at spots along the North Atlantic Current path, and some strong warming near the southern tip of Japan (which also has some expression at most depths, but is much weaker at 500 m). There are some regions where the temperature trend has the same sign at different depths—notably, the central North Pacific near 40°N, the cooling right off of Newfoundland near 50°N, and the previously mentioned regions. In other locations, there is vertical structure to the trends, with suggestions of warming in the Indian Ocean and the western South Pacific at upper depths to cooling at middle depths. Vertical structure is also suggested off the coast of California, around Cuba, and in the South Atlantic.

The regions satisfying the data distribution requirement for each grid cell of three or more observations for four of the five "decades" (here 9.8-yr periods) on the 3° × 3° grid are shown in Fig. 5. No new information is contained in this figure that is not in Fig. 4 except for noisy regions (regions of high box-to-box trend variability), and regions of weak trends that somewhat connect regions of oppositely signed stronger trends. The maps in Fig. 5 clearly show a strong reduction in coverage with depth, which here is due to the lack of data coverage through time in much of the ocean at deeper depths. These maps are a consequence of the sampling issues shown above in Fig. 1 and extend the similar results in HC.

3.3 Comparison to WOD05 standard-level data

The results presented above are all calculated from binned and gridded observed-level data from WOD05. In this section we compare these results to trends calculated from standard-level data available in WOD05. The standard-level data are observations interpolated to standard depths, so no bin sizes are needed for depth. This procedure tends to give more points in any grid box over any time interval in question compared to depth-binning of observed-level data, which yields better spatial coverage of long-term trends. Maps of these trends are presented in Fig. 6 for the 1955–2003 period. To make the maps comparable, the standard-level data were gridded into 3° × 3° boxes. The trend noise in the Antarctic Circumpolar Current region of the Southern Hemisphere is still distinguishable by high small-scale spatial variability, particularly south of 40°S at the upper depths, and appearing more in subtropical regions of the southern basins at lower depths (Figs. 6d, e,

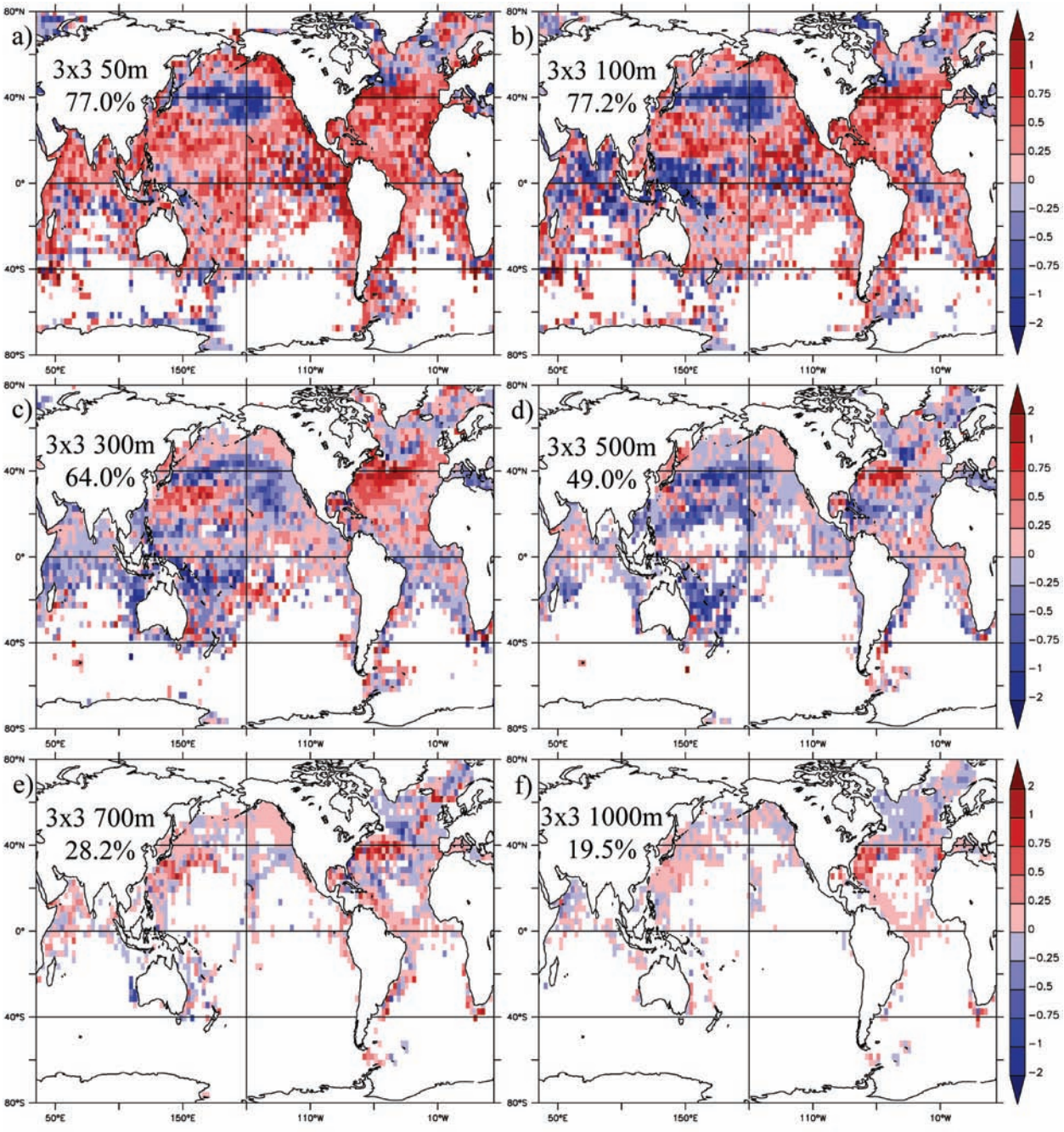

Figure 5: Same as Fig. 4 except for all regions passing the sampling criterion.

f). Note that no data distribution or statistical significance filter has been applied to these results.

Just like for the observed-level data trends, there are large-scale coherent patterns of trends in the Northern Hemisphere and in parts of the tropics in Fig. 6. The same patterns are produced as with the observed-level data (difference map shown in Fig. 7; constructed from Fig. 6 trend magnitudes minus Fig. 5 magnitudes) with a few notable exceptions. There are some warming and cooling differences at 50 m in the eastern tropical Pacific, with some weaker differences there at 100 m (Figs. 7a, b). This is an area which is particularly undersampled, in addition to the southern ocean basins. Also, the cooling in the East Indian and warming north of Papua New Guinea at 100 m is stronger here (Fig. 7b). Regions of stronger warming and weaker cooling include the North Pacific basin at 500 m, along with the much weaker cooling in the South Pacific east of Australia (Fig. 7d). These differences would increase the trend of the heat content integral significantly, but elsewhere the patterns match up well with the observed-level trend patterns, even in magnitude. It appears that the process of interpolating data to standard levels does not reproduce quite the same trend patterns that binning over a depth range does, but the differences are mostly regional and usually small, with the exceptions above.

3.4 Comparison to LEV05 dataset

The dataset analyzed in Levitus *et al.* (2005) was obtained from the NODC website and trends were calculated from it at the depths previously discussed for comparison. The results are displayed in Fig. 8 and do not include 1000 m, since the analysis only went as deep as the 700 m standard level. Superficially, the LEV05 trends bear a semblance of the same kinds of trend patterns evident in the standard- and observed-level data. It does contain large-scale coherent trends with similar sign to the above results in many regions. However, the warming regions look to be stronger at the upper depths, and the region along 40°N east of North America looks very strongly warming at all depths. Also, the Southern Ocean, and all southern ocean basins south of 40°S, mostly have weaker trends than regions north of there. It is clear that the smoothing procedures used to build this dataset produce weaker and less noisy trend variability in this region. This suggests that while the objective analysis procedure dampens out noise in the southern ocean regions, stronger trend patterns do not emerge from the lack of sampling there.

It is easier to compare the LEV05 trend results to the observed- and standard-level data trend results by constructing difference maps. Due to the LEV05 dataset already having been smoothed, the trend difference maps have been smoothed to a similar degree to keep the maps as readable as possible. The difference maps were calculated by subtracting the standard-level and observed-level $3° \times 3°$ trend magnitude maps (Figs. 5 and 6), regridded onto a $1° \times 1°$ grid, from the $1° \times 1°$ LEV05 trend magnitude maps (Fig. 8). Before smoothing, any unrealistic trends above a cutoff of $\pm 4°\mathrm{C} \cdot (49\ \mathrm{yrs})^{-1}$

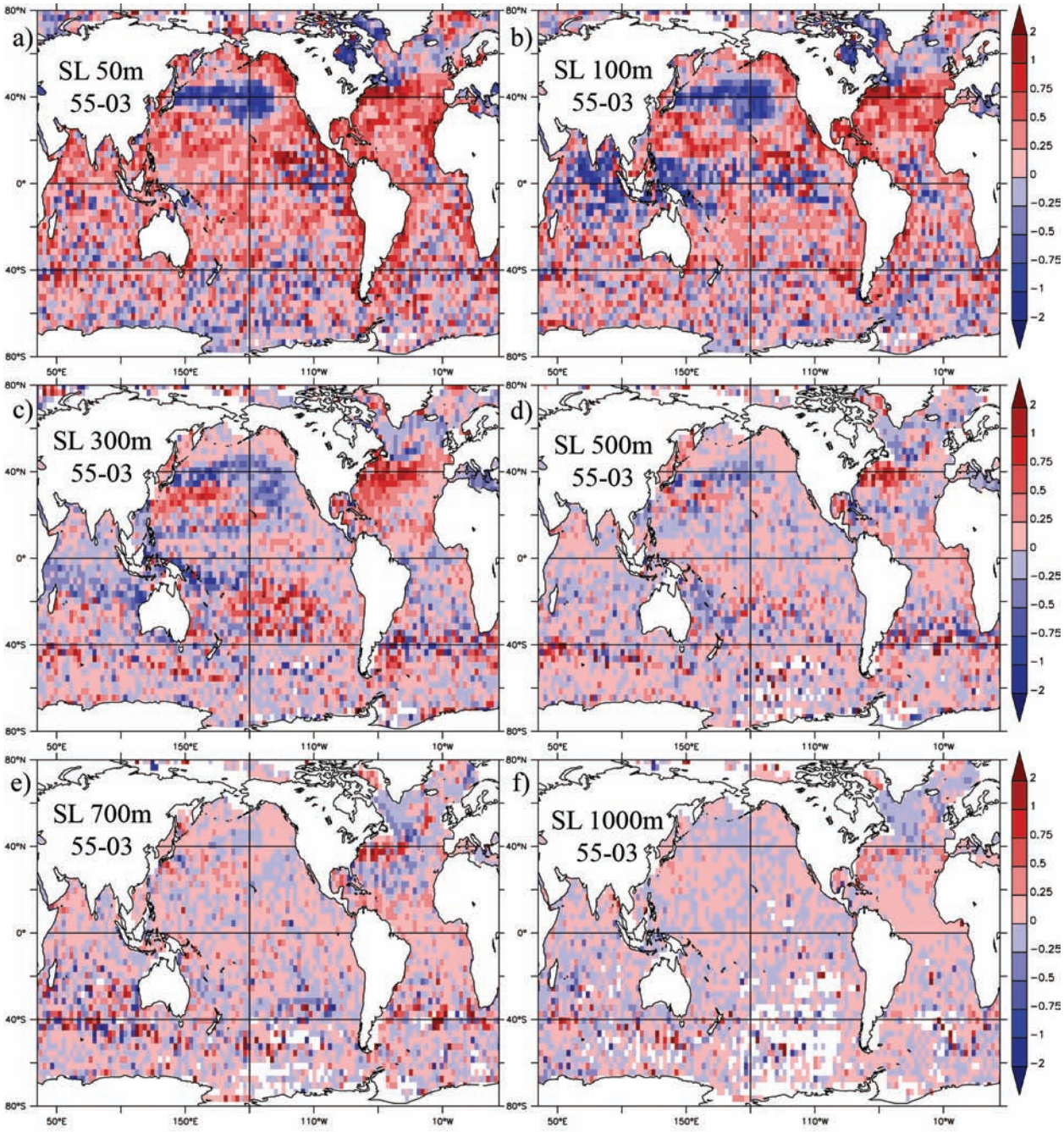

Figure 6: Temperature trends based on WOD05 standard-level (SL) anomalies over the period 1955–2003 (units are °C per 49 years). Shown are all regions with data. The standard-level depth for each panel is listed in Asia. The data were gridded to a 3° × 3° grid. The color bar is the same as in previous trend figures.

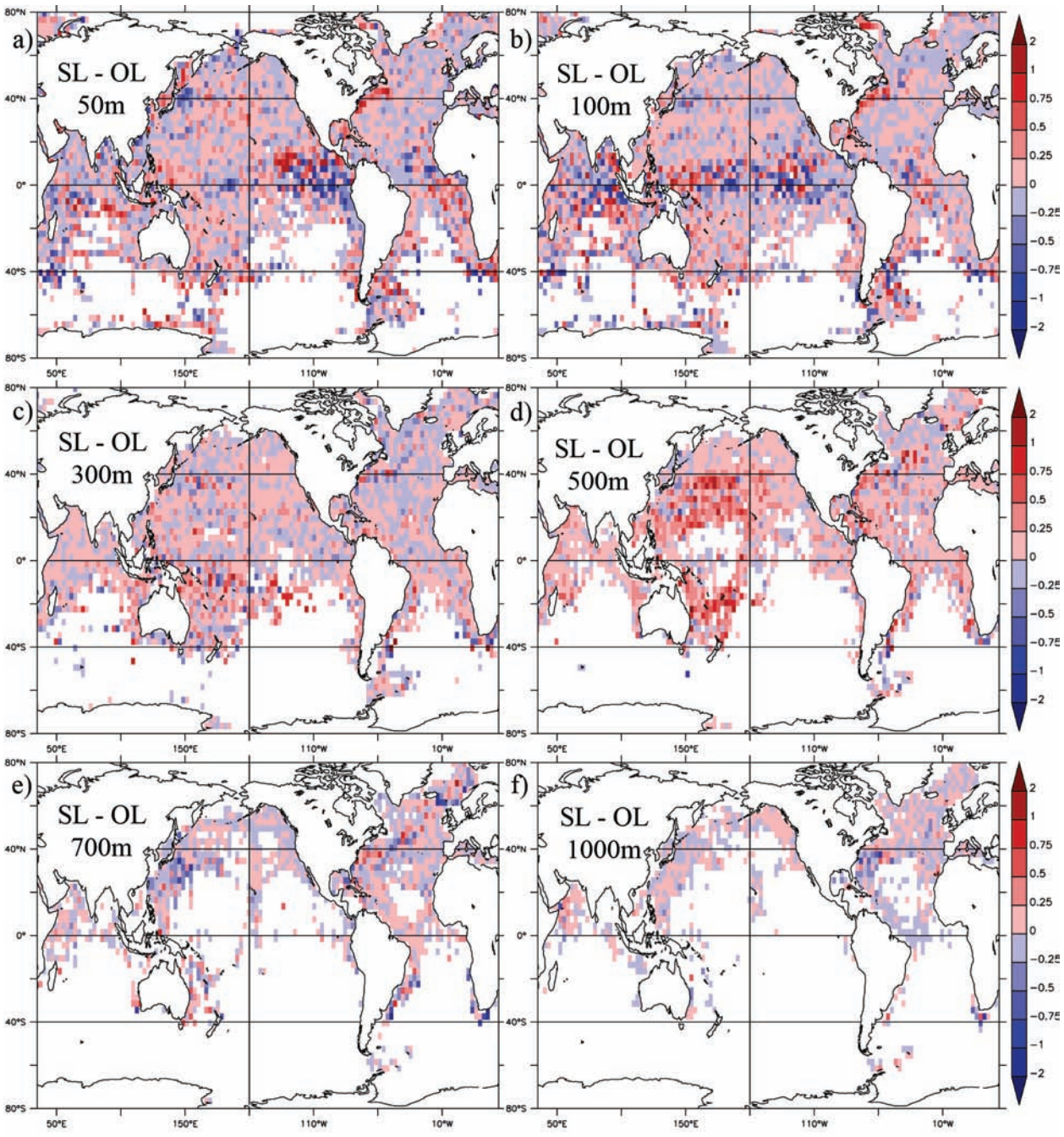

Figure 7: Temperature trend differences (in units of °C per 49 years) for the WOD05 standard-level (SL) trends minus the WOD05 observed-level (OL) trends (both on 3° × 3° grid). The standard-level depth for each panel is listed in Asia. The color bar is the same as in previous trend figures.

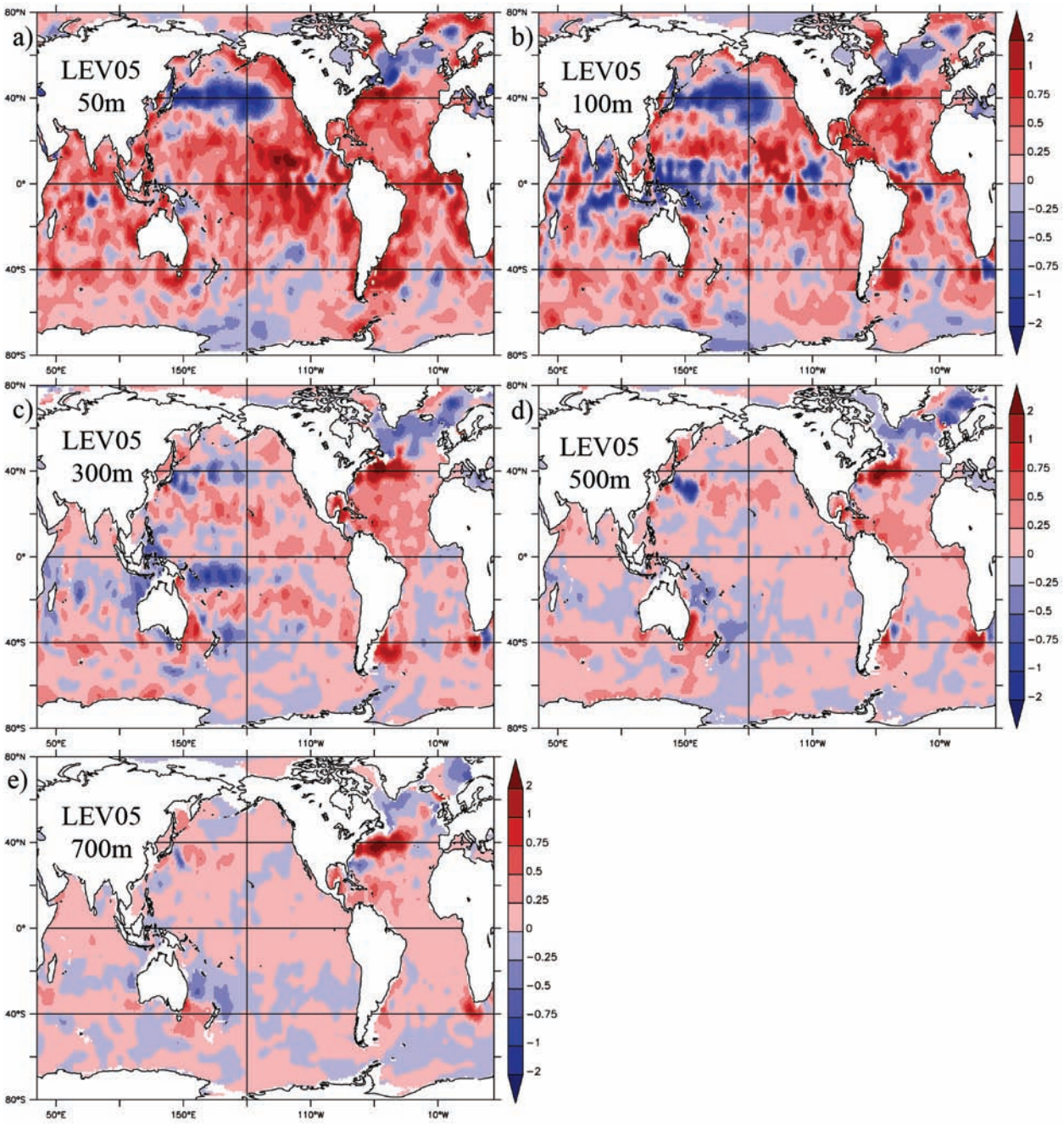

Figure 8: Temperature trends based on the objectively analyzed temperature anomaly dataset (LEV05) examined in Levitus *et al.* (2005). The data in LEV05 are all yearly temperature anomalies on a $1° \times 1°$ grid. The trends are over the period 1955–2003 (in units of °C per 49 years). The standard-level depth for each panel is listed in Asia. These maps show trends based on the original data and are not smoothed any further here. The color bar is the same as in previous trend figures.

were filtered out in order to keep tiny regions with very large trends from contaminating the smoothed maps. These were then smoothed with a Welch window applied to nearest neighbors in longitude and latitude—which has weights of {0.3, 0.4, 0.3} (see, e.g., Press *et al.*, 1992). Since the important differences are large scale, this does not pose a problem; the smoothed maps are qualitatively the same as the unsmoothed maps (not shown).

The differences between LEV05 and the WOD05 standard-level data trends are presented in Fig. 9. Note that the noise in the southern regions of the Southern Hemisphere is still present in these maps and it comes from the noise in the standard-level data maps. The differences in the upper layers (50 and 100 m) include the stronger warming (darker reds) in LEV05 trends over much of the Indian Ocean and the Tropics (Figs. 9a, b). Stronger warming also occurs in much of the subtropical South Atlantic, subtropical North Atlantic, central North Pacific, and between Argentina and the Antarctic Peninsula. The LEV05 trends are less warming along the coast of northern Africa and in the subpolar regions of the North Atlantic. There is also some broad scattered cooler difference in much of the midlatitude North Pacific.

At the deeper depths (Figs. 9c, d, e), the very strong warming along 40°N east of North America in the LEV05 trends overpowers any similar warming in the standard-level trends. There is also stronger warming in LEV05 over much of the central North Pacific and the Tropics, especially near Florida and the Caribbean. While there are still regions of more cooling or less warming trends in the subpolar and subtropical North Atlantic and North Pacific, the warming regions are stronger and cover more area on average.

The difference maps comparing the LEV05 trends to the observed-level trends are shown in Fig. 10. These maps strongly suggest a warming bias between the LEV05 trends and the observed-level trends. The upper layer trends (Figs. 10a, b) in LEV05 have more positive slope in most places except in the eastern and northern North Atlantic and the western and northwestern North Pacific. There are also pockets of more negative slope relative to the observed-level trends in the eastern tropical Pacific, but there are more and stronger pockets of positive slope throughout this region. Certainly, this is one of the more undersampled regions outside of the southern ocean basins. At deeper depths, the warming bias is widespread and dominates all basins (Figs. 10c, d, e), although at 700 m the stronger LEV05 warming is mostly confined to the same North Atlantic region along 40°N.

3.5 Overlapping 20-year trends from WOD05

Another extension of the results in HC is the maps of overlapping 20-year trends—composed of data from WOD05, calculated as monthly anomalies, and gridded into the $2^\circ \times 10^\circ$ boxes for the best possible spatial coverage. Regions masked out are ones that do not pass the data distribution requirement for each grid cell and therefore do not likely have enough data to calculate 20-year trends for all periods.

Figure 11 shows the 20-year trends at 100 m for the periods: January 1955 to January 1975, 1960–1980, 1965–1985, 1970–1990, 1975–1995, and

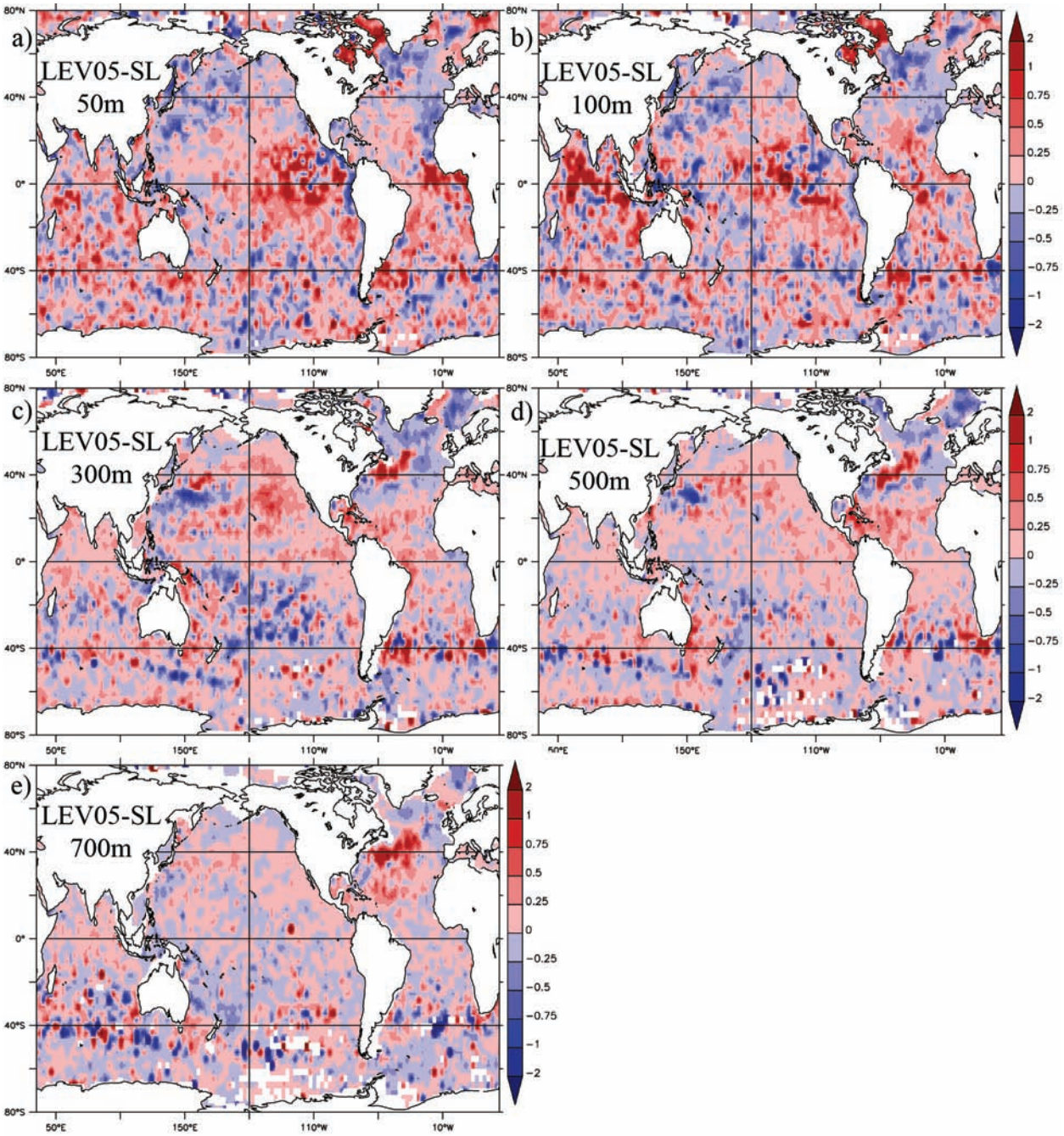

Figure 9: Temperature trend differences (in units of °C per 49 years) for the LEV05 dataset trends minus the WOD05 standard-level (SL) trends (regridded to $1° \times 1°$). The standard-level depth for each panel is listed in Asia. The difference map was smoothed by a Welch window which included nearest neighbors in both longitude and latitude to improve readability. The color bar is the same as in previous trend figures.

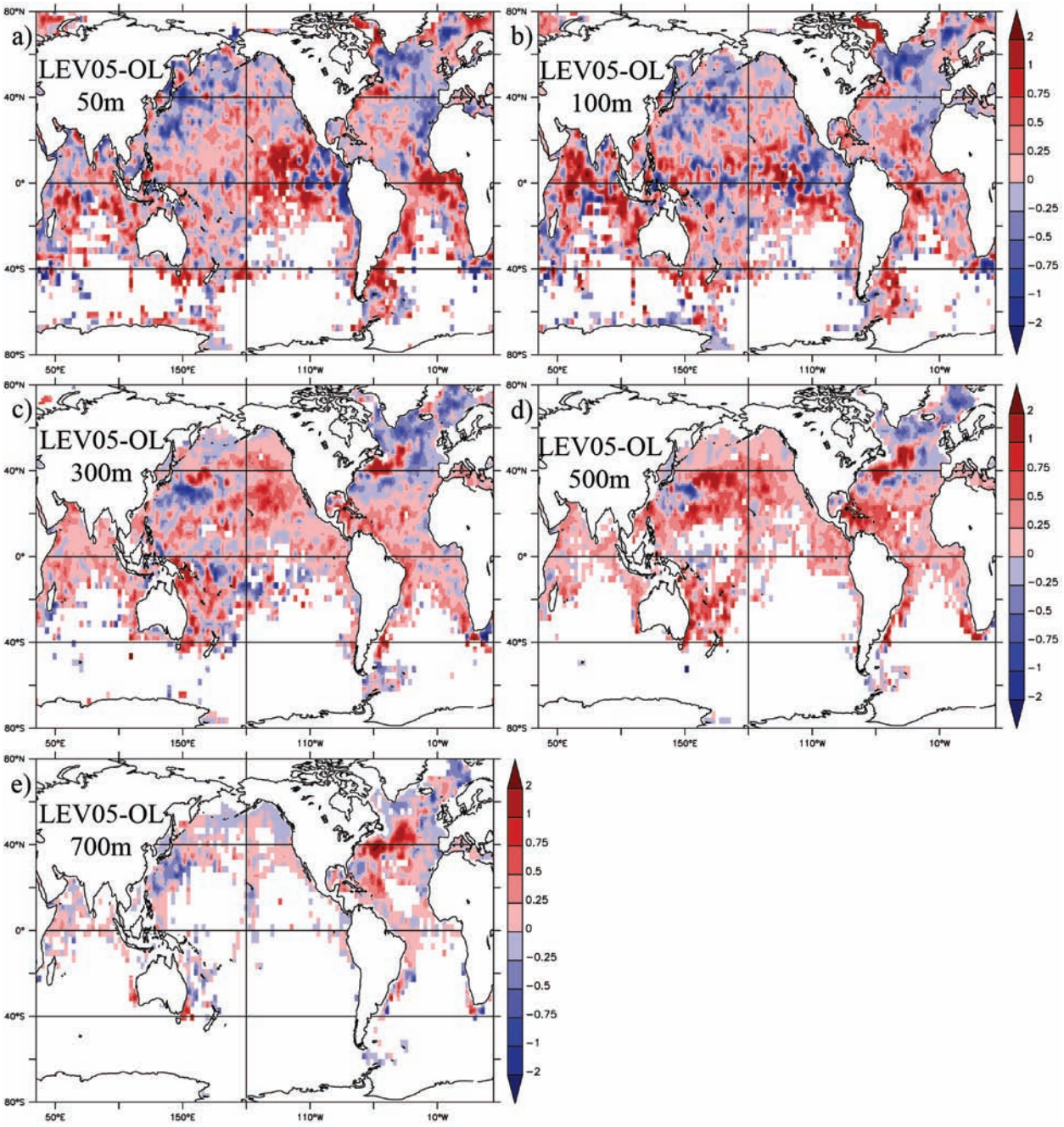

Figure 10: Same as Fig. 9 except temperature trend differences are LEV05 dataset trends minus the WOD05 observed-level (OL) trends described in the text. The grid size for the WOD05 data is $3° \times 3°$ (regridded to $1° \times 1°$ to match LEV05), and the resulting difference maps were smoothed as in Fig. 9.

1980–2000. More of the ocean is covered by regions passing the data distribution requirement on this grid than on the HC 2° × 2° grid. These regions, which are mostly in the Southern Hemisphere, are much more poorly sampled in the early part of the records than the Northern Hemisphere, as described above. Thus the early trends in these basins are mostly noise, with high box-to-box variability. The later trends (Figs. 11d, e, f) still lack large coherent regions of trends south of 40°S, although there still appears to be interdecadal signals in many of these regions. For the southern tropics and subtropics, there is evidence of interdecadal variability in the South Pacific and South Atlantic in the last four panels of Fig. 11.

The broad coherent patterns of temperature trends in the Northern Hemisphere basins are reproduced again, and show no substantial difference from the patterns reported in HC. Some details, however, can be significantly different due to the difference in data analysis approach, especially in the early panels where trends are based on fewer points.

The 20-year trends at 300 and 500 m (Figs. 12 and 13, respectively) display a nearly global interdecadal signal of trend sign and strength. After the first two panels in both figures (where the number of points upon which to base a trend are fewest), there is a surprising number of regionally coherent trend patterns that shift from warming to cooling, or vice versa, between the 1965–1984 trends and the 1980–1999 trends. In the earliest two panels, there are many regions of strong warming which subsequently pass into regions of cooling in later periods. These patterns, particularly striking at 500 m (Fig. 13), appear to be the spatial expression of the strong warming period at these middle depths in the 1970s and 1980s as reported in Levitus *et al.* (2000, 2005), and discussed in Gregory *et al.* (2004), Levitus *et al.* (2005), and Gouretski and Koltermann (2007).

4. Summary and Discussion

The basic results of HC have been shown to be largely unaffected by applying a slightly weaker data distribution requirement and working with temperature anomalies relative to a climatology, thereby permitting the use of larger analysis box sizes. Even though more of the world ocean satisfies the weaker data criterion with larger box sizes, few new geographical regions have statistically significant trends. At 2° × 10° analysis box resolution, the area of the global ocean between 80°S and 80°N containing significant 50-year trends is 38.1% for 50 m, 36.3% for 100 m, 27.7% for 300 m, and 19.6% at 500 m. These trends exhibit sub-basin scale patterns of large warming and cooling (peak amplitudes in excess of 1.5°C). Further, there is comparable variability in running 20-year trend estimates; almost all of the analysis regions had both warming and cooling 20-year trends over a 50-year period. Thus the analysis reveals an upper ocean with much interdecadal trend variability in space and time. It is difficult even to say how well the statistically significant 50-year trend patterns will turn out to characterize longer-term upper oceanic trends.

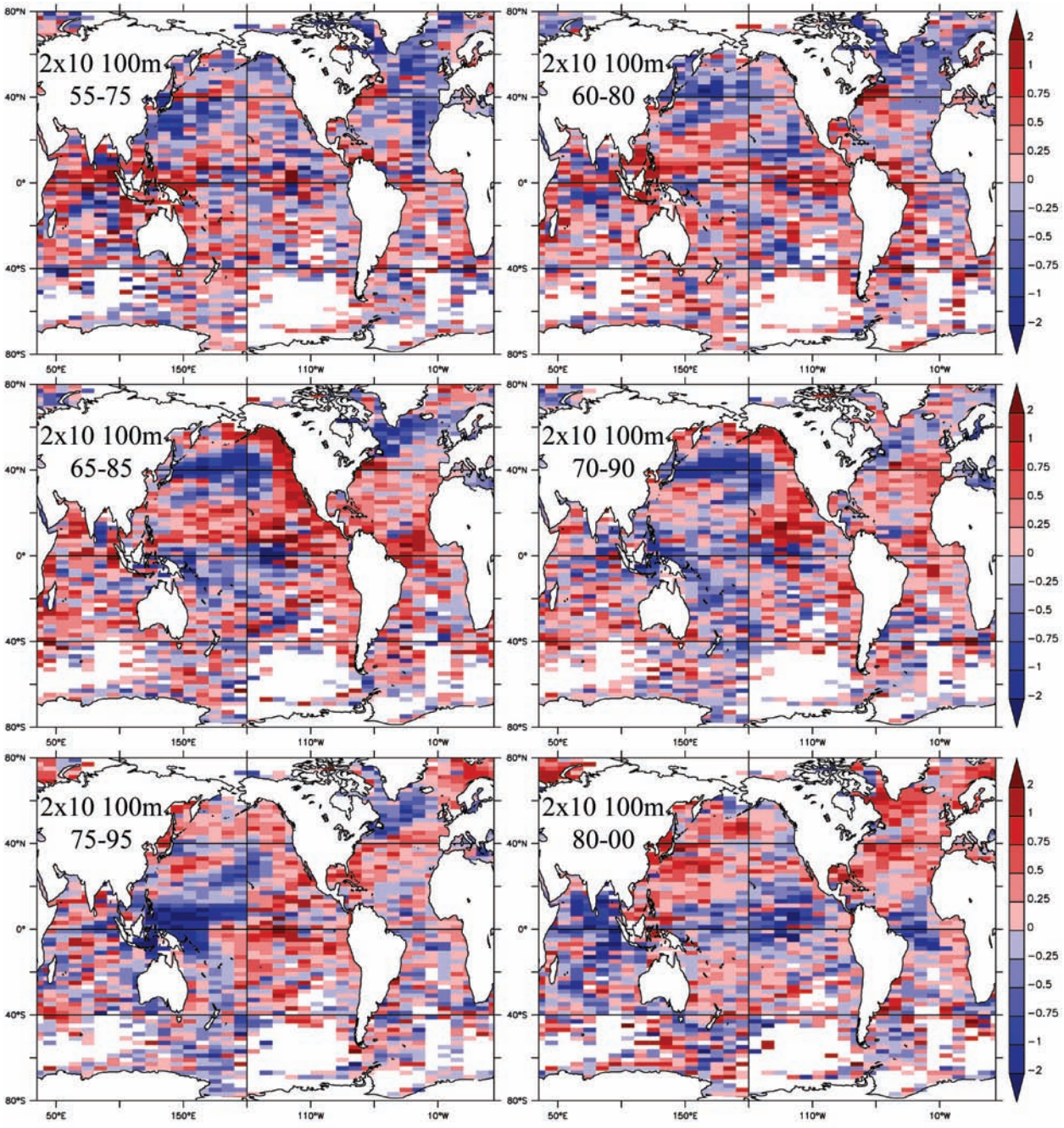

Figure 11: 20-year temperature trends (in °C per 20 years) for 2° latitude by 10° longitude regions at 100 m. The time periods covered are listed in Asia in each box and run from January of the first year through January of the last year. Trends are shown for all regions satisfying the sampling criterion. The color bar is the same as in previous trend figures.

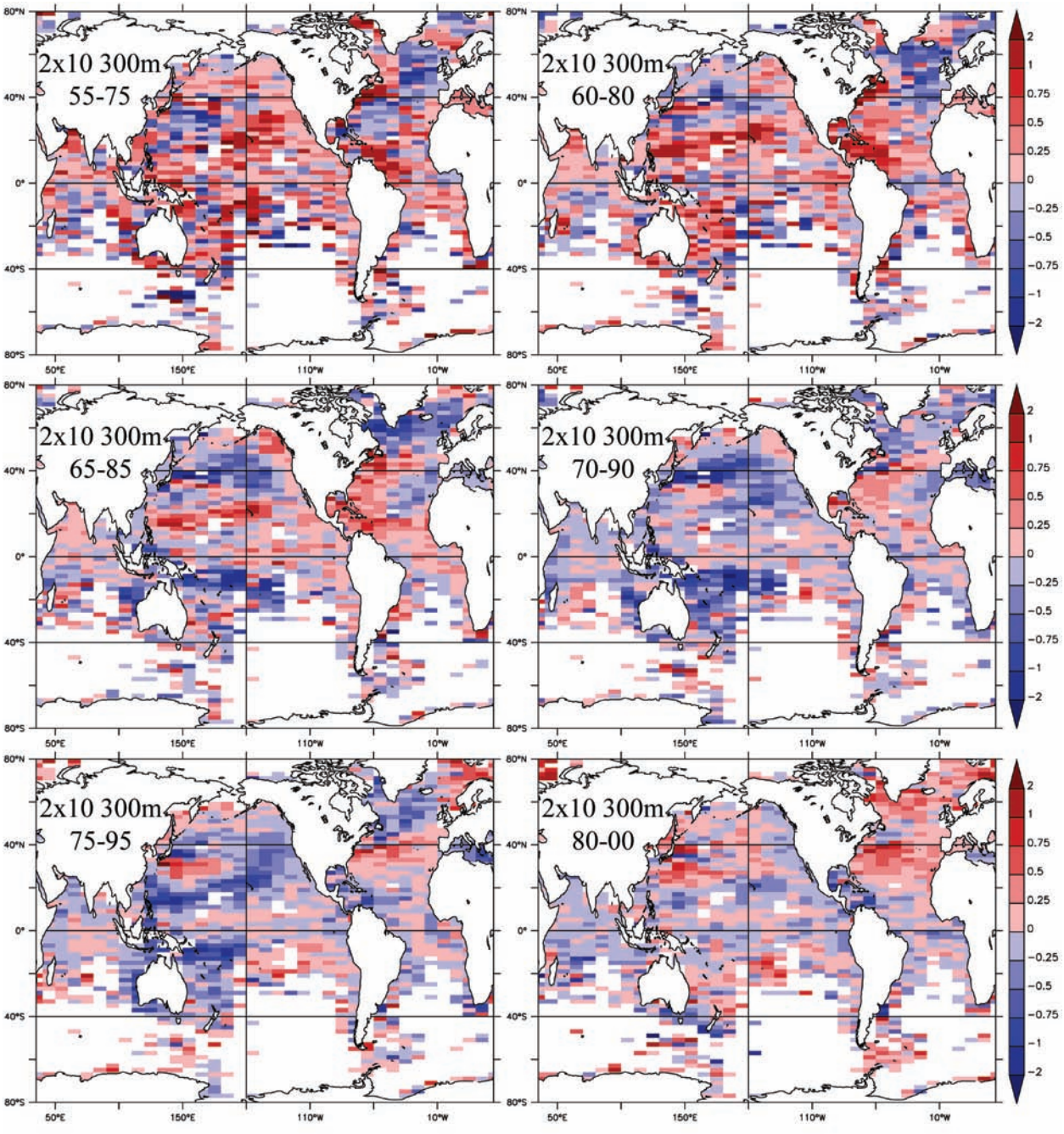

Figure 12: Same as Fig. 11 except for 300 m.

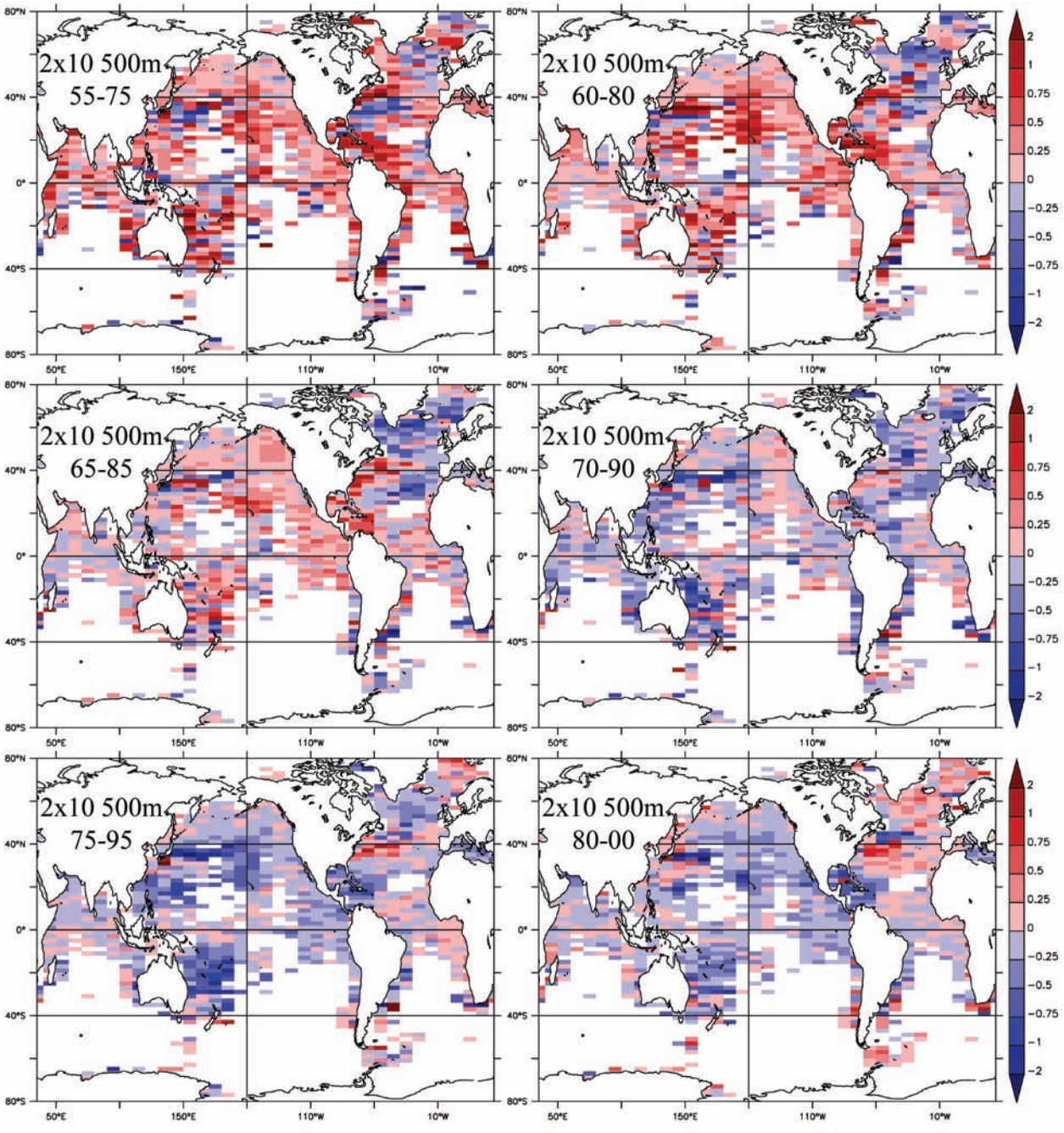

Figure 13: Same as Fig. 11 except for 500 m.

Detection of global ocean trends from these results is not simple. Some of the trend variance almost certainly represents advective redistribution of heat within the ocean. Detection of global trends would be simplified if volume averaging could be done to account for advection. There are several challenges to this. The first is that the historical data distribution reveals the ocean has been very non-uniformly sampled in time and space. Most of the observations have been collected in the later part of the 1955–2003 interval, and most have been collected in the Northern Hemisphere near coasts. Any volume integration thus depends first upon making some sort of interpolation/extrapolation to fill the vast data-poor parts of the ocean.

The consequences of these sampling biases on estimates of 50-year trends based on interpolated fields have been shown by considering three different datasets, all of which are based on the same raw data. These have significantly different trend patterns in many areas due to the different data analysis methods. The LEV05 dataset, which is the most smoothed of the three, yields warmer trends over the 1955–2003 interval in many parts of the ocean and at many depths than do the standard-level trends from WOD05, and much warmer trends than the observed-level trends from our analyses. Striking differences occur even in some regions where there are statistically significant trends.

Vertical integration over different depth ranges (e.g., 0–300 m, 0–700 m) and often over oceanic basins has been used to simplify analysis (Levitus *et al.*, 2005; Lyman *et al.*, 2006, and others). The results presented here suggest that the needed interpolation in space may have substantial effects on these results. In particular, they suggest that the heat content trend estimates presented in Levitus *et al.* (2005) may be an upper limit.

Others have considered aspects of the sampling implications for long-term trend estimation. Uncertainty due to sampling issues beneath the depths of XBTs (∼700–1000 m) has been considered by Gouretski and Koltermann (2007), who estimate over a 50% sampling error range for the heat content estimates of the 0–3000 m layer. Also, Lyman *et al.* (2006) estimated the 0–750 m sampling error by applying the spatio-temporal sampling patterns in the individual years 1955–2005 to the satellite altimeter data from AVISO (an upper-ocean heat content proxy) and found that the sampling error prior to 1967 is much greater than after, when XBTs became available. Their error estimate suggests that upper-ocean heat content trends using data prior to 1967 are susceptible to large errors.

The large temperature variability of the global ocean, coupled with strongly biased temporal and spatial sampling, yields datasets that are incomplete in their description of the evolution of the ocean state. Trends are susceptible to differences in data processing techniques used to produce a final data product. The issues of data-comparability from different instruments, raised by Gouretski and Koltermann (2007), may also introduce non-trivial uncertainty. Because of these challenges, we suggest that it is very important to look carefully at uncertainty estimates for world ocean

heat content (and temperature) trends, and there should be continuing efforts in this field.

5. Acknowledgments

This work was supported by the NOAA Office of Climate Observations and NOAA's Pacific Marine Environment Laboratory, Eddie Bernard, Director. Much of the work presented here was obtained with the freeware analysis package, Ferret, `http://www.ferret.noaa.gov`.

6. References

Barnett, T.P., D.W. Pierce, K.M. AchutaRao, P.J. Gleckler, B.D. Santer, J.M. Gregory, and W.M. Washington (2005): Penetration of human-induced warming into the world's oceans. *Science*, *309*, 284–287.

Boyer, T.P., *et al.* (2006): World Ocean Database 2005. NOAA Atlas NESDIS 60, S. Levitus (ed.), NOAA, U.S. Government Printing Office, Washington, D.C., 190 pp., DVDs.

Conkright, M.E., *et al.* (2002): Introduction. Vol. 1, World Ocean Database 2001, NOAA Atlas NESDIS 42, NOAA, 160 pp.

Gille, S.T. (2002): Warming of the Southern Ocean since the 1950s. *Science*, *295*, 1275–1277.

Gouretski, V., and K.P. Koltermann (2007): How much is the ocean really warming? *Geophys. Res. Lett.*, *34*, L01610, doi:10.1029/2006GL027834.

Gregory, J.M., H.T. Banks, P.A. Stott, J.A. Lowe, and M.D. Palmer (2004): Simulated and observed decadal variability in ocean heat content. *Geophys. Res. Lett.*, *31*, L15312, doi:10.1029/2004GL020258.

Hanawa, K., P. Rual, R. Bailey, A. Sy, and M. Szabados (1995): A new depth time equation for Sippican or TSK T-7, T-6 and T-4 expendable bathythermographs (XBT). *Deep-Sea Res.*, *42*, 1423–1451.

Harrison, D.E., and M. Carson (2007): Is the world ocean warming? Upper-ocean temperature trends: 1950–2000. *J. Phys. Oceanogr.*, *37*, 174–187.

Levitus, S., J.I. Antonov, and T.P. Boyer (2005): Warming of the world ocean, 1955–2003. *Geophys. Res. Lett.*, *32*, L02604, doi:10.1029/2004GL021592.

Levitus, S., J.I. Antonov, T.P. Boyer, and C. Stephens (2000): Warming of the world ocean. *Science*, *287*, 2225–2229.

Levitus, S., T. Boyer, and J. Antonov (1994): Interannual variability of upper ocean thermal structure. Vol. 5, World Ocean Atlas 1994, NOAA Atlas NESDIS 5, NOAA, 176 pp.

Locarnini, R.A., A.V. Mishonov, J.I. Antonov, T.P. Boyer, and H.E. Garcia (2006): Temperature. Vol. 1, World Ocean Atlas 2005, NOAA Atlas NESDIS 61, NOAA, 182 pp.

Lyman, J.M., J.K. Willis, and G.C. Johnson (2006): Recent cooling of the upper ocean. *Geophys. Res. Lett.*, *33*, L18604, doi:10.1029/2006GL027033.

Pierce, D.W., T.P. Barnett, K.M. AchutaRao, P.J. Gleckler, J.M. Gregory, and W.M. Washington (2006): Anthropogenic warming of the oceans: Observations and model results. *J. Climate*, *19*, 1873–1900.

Press, W.H., B.P. Flannery, S.A. Teukolsky, and W.T. Vetterling (1992): *Numerical Recipes in FORTRAN: The Art of Scientific Computing*. Cambridge University Press, 992 pp.

Willis, J.K., D. Roemmich, and B. Cornuelle (2004): Interannual variability in upper ocean heat content, temperature, and thermosteric expansion on global scales. *J. Geophys. Res.*, *109*, C12046, doi:10.1029/2003JC002260.

Appendix A.

To aid in comparing the current results with the results of Harrison and Carson (2007), Fig. 7 from that paper has been reprinted here as Fig. A1 using the color scheme adopted for the results in the current paper. The new analysis differs from the one in HC by using WOD05 observed-level data instead of WOD01, removing the monthly climatological means (from WOA05) from the raw data before gridding and calculating monthly anomaly averages, and applying the XBT correction of Hanawa *et al.* (1995) to the instruments identified using the criteria discussed in Section 2 above. The results in HC were based on gridded daily averages with no climatological means removed and no XBT corrections applied. The points of comparison would be Fig. 2a to Fig. A1a, Fig. 2e to Fig. A1b, Fig. 3a to Fig. A1d, and Fig. 3e to Fig. A1e.

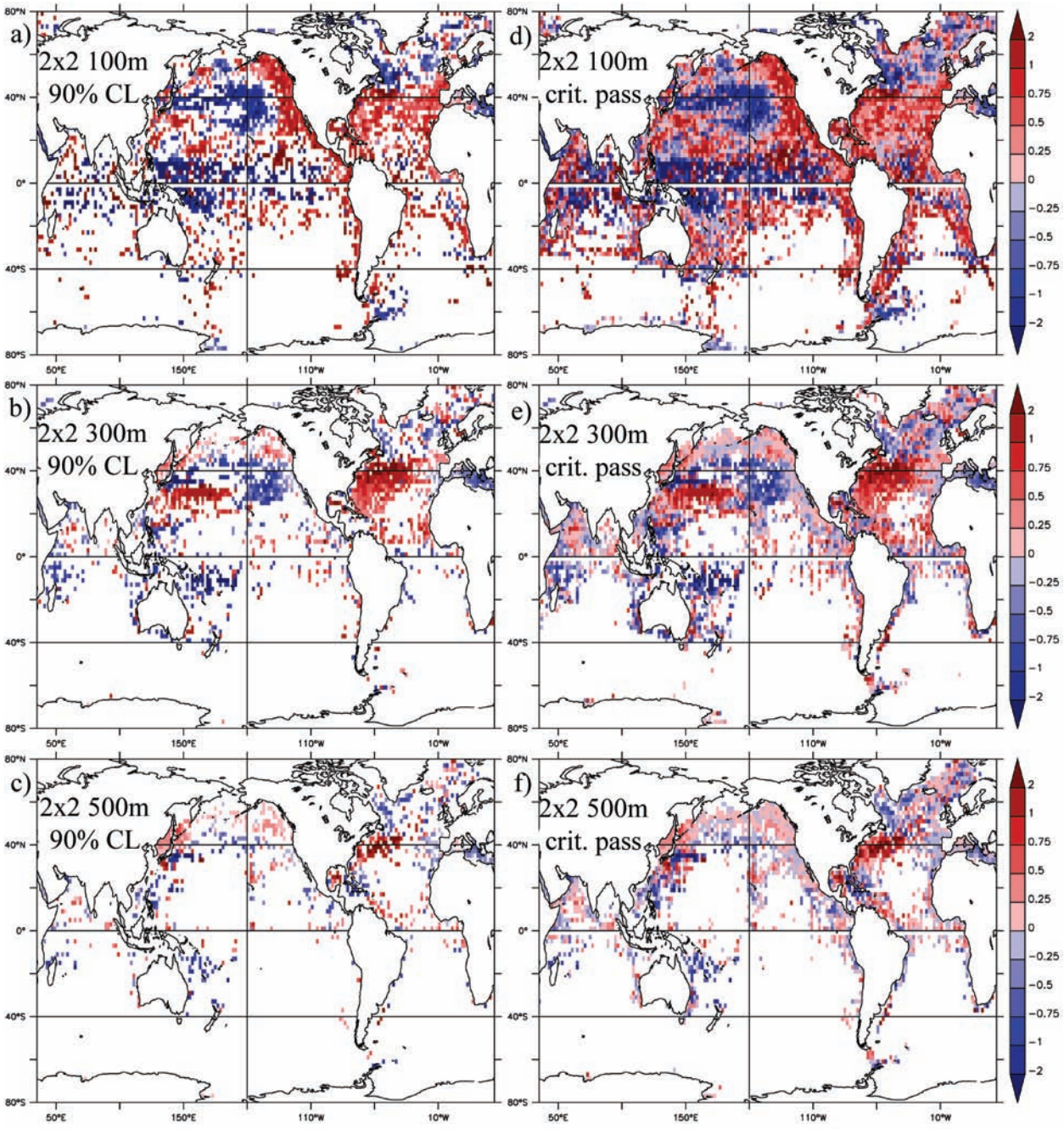

Figure A1: From Fig. 7 of Harrison and Carson (2007) with the color bar for trend magnitudes adopted for use in the present paper. Units are °C per 51 years.